Diagn Interv Radiol 2014; 20:438–447

MOLECULAR IMAGING
REVIEW

Clinical applications of PET/MRI: current status and future perspectives

Felix Nensa, Karsten Beiderwellen, Philipp Heusch, Axel Wetter

ABSTRACT
Fully integrated positron emission tomography (PET)/magnetic resonance imaging (MRI) scanners have been available for a few years. Since then, the number of scanner installations and published studies have been growing. While feasibility of integrated PET/MRI has been demonstrated for many clinical and preclinical imaging applications, now those applications where PET/MRI provides a clear benefit in comparison to the established reference standards need to be identified. The current data show that those particular applications demanding multiparametric imaging capabilities, high soft tissue contrast and/or lower radiation dose seem to benefit from this novel hybrid modality. Promising results have been obtained in whole-body cancer staging in non-small cell lung cancer and multiparametric tumor imaging. Furthermore, integrated PET/MRI appears to have added value in oncologic applications requiring high soft tissue contrast such as assessment of liver metastases of neuroendocrine tumors or prostate cancer imaging. Potential benefit of integrated PET/MRI has also been demonstrated for cardiac (i.e., myocardial viability, cardiac sarcoidosis) and brain (i.e., glioma grading, Alzheimer's disease) imaging, where MRI is the predominant modality. The lower radiation dose compared to PET/computed tomography will be particularly valuable in the imaging of young patients with potentially curable diseases.
However, further clinical studies and technical innovation on scanner hard- and software are needed. Also, agreements on adequate refunding of PET/MRI examinations need to be reached. Finally, the translation of new PET tracers from preclinical evaluation into clinical applications is expected to foster the entire field of hybrid PET imaging, including PET/MRI.

From the Department of Diagnostic and Interventional Radiology and Neuroradiology (F.N. ✉ *felix.nensa@gmail.com*, K.B., A.W.), University Hospital Essen, University of Duisburg-Essen, Essen, Germany; the Department of Diagnostic and Interventional Radiology (P.H.), University Hospital Dusseldorf, University of Dusseldorf, Dusseldorf, Germany.

Received 8 January 2014; revision requested 7 February 2014; revision received 3 March 2014; accepted 13 April 2014.

Published online 19 June 2014.
DOI 10.5152/dir.2014.14008

Both positron emission tomography (PET) and magnetic resonance imaging (MRI) are well-established imaging modalities that have been clinically available for more than 30 years. However, the combination of PET and computed tomography (CT) into PET/CT has heralded a new era of hybrid imaging driven by the rapid ascend of PET/CT and the decline of stand-alone PET. The integration of PET and CT into a hybrid system provided added value that exceeds the sum of its parts, in particular fast and accurate attenuation correction and the combination of anatomical and molecular information.

Inspired by the vast success of PET/CT, the combination of PET and MRI was an obvious goal. Therefore initial solutions comprised the software based co-registration and post-hoc fusion (1) of independently acquired PET and MRI data, as well as shared tabletop sequential PET and MRI acquisition (2, 3). While the integration of PET and CT into a hybrid system was challenging but technically feasible, the integration of PET and MRI was considered extremely demanding, if not impossible. Two main technical challenges that had to be solved: in the first place development of a PET insert that is compatible to high magnetic field strengths normally used in MRI, and vice versa development of a magnetic resonance (MR) scanner that guarantees a stable and homogenous magnetic field in the presence of a PET insert. Conventional PET detectors consist of scintillation crystals and photomultipliers, and the latter, being very sensitive to magnetic fields, cannot be used in integrated PET/MRI systems. Hence, one approach was to replace photomultipliers by avalanche photodiodes (APDs), which are insensitive to even strong magnetic fields (4). The scintillation crystals used in PET/MRI scanners are usually composed of lutetium ortho-oxysilicate, with the advantage of only minor disturbances of magnetic field homogeneity (Fig. 1). Next generation PET/MRI scanners could be based on silicon photomultiplier PET detectors, which showed better performance characteristics than the APDs and, in contrast to these, are capable of time-of-flight imaging (5). Secondly, the development of MR-based attenuation correction methods is necessary, as the commonly used method for attenuation correction in PET/CT systems, which is based on the absorption of X-rays, is not transferable to MRI. Hence, different methods for attenuation correction in PET/MRI systems have been proposed, one of which consists of segmentation of the attenuation map into four classes (background, lung tissue, fat, and soft tissue) (6). In principle, the MR-based attenuation map is created with a two-point Dixon sequence (7), providing water-only and fat-only images, which are combined and segmented to form an MR-based attenuation map. The method proved its technical feasibility with the limitation that in bone tissue and in its vicin-

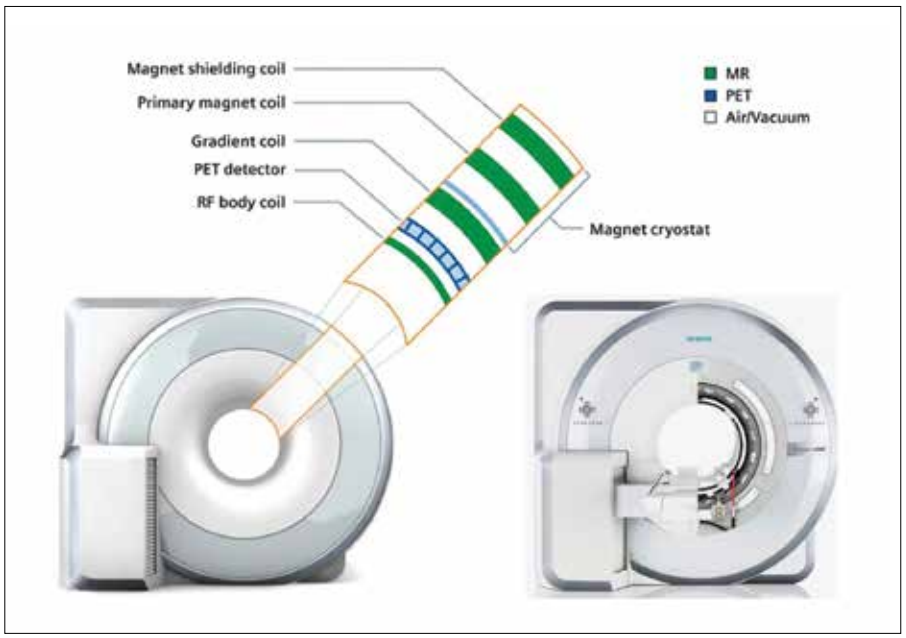

Figure 1. Diagram of an integrated PET/MRI scanner with capability of simultaneous PET and MRI data acquisition. Image courtesy of Siemens Healthcare, Erlangen, Germany.

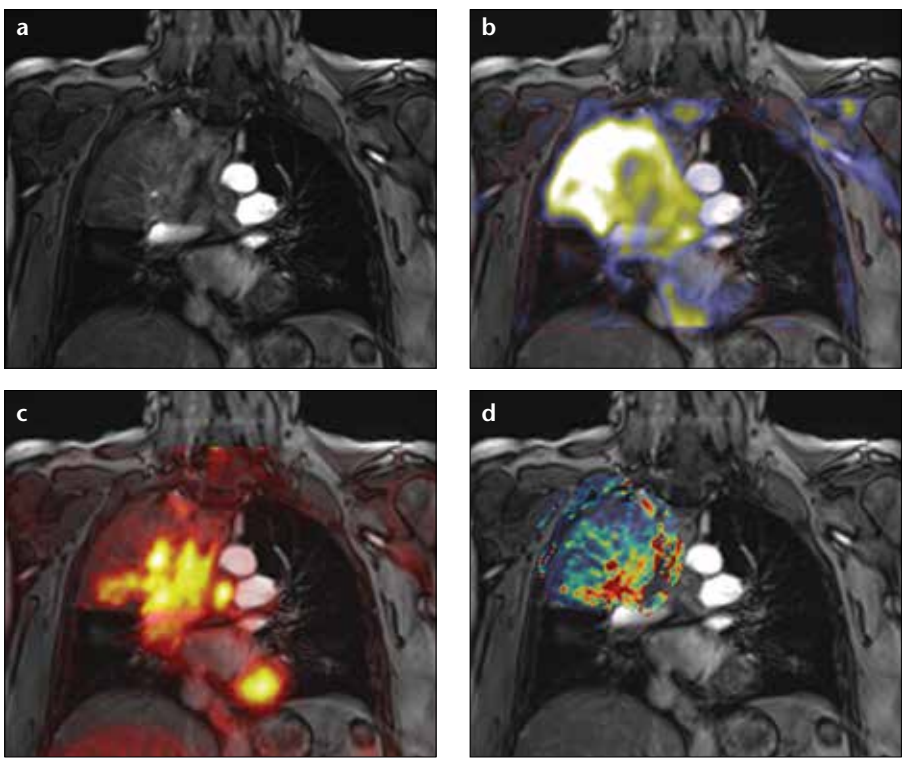

Figure 2. a–d. Multiparametric simultaneous PET/MRI in a patient with non-small cell lung cancer of the right upper lobe. The contrast-enhanced T1-weighted coronal image **(a)** is fused with the apparent diffusion coefficient **(b)**, FDG-PET **(c)** and dynamic contrast-enhanced derived transfer coefficient (**d**). Multiparametric PET/MRI allows for a more holistic understanding of tumor and tumor stroma, potentially enabling better cancer characterization and therapy control.

ity standardized uptake values (SUV) derived from PET/MRI systems might be erroneously underestimated when compared to SUVs derived from PET/CT (8). Therefore, SUVs derived from PET/MRI systems should be interpreted carefully until a larger experience with the new method of PET/MRI exists.

In 2010, the first fully integrated whole-body PET/MR hybrid imaging system based on APD technology and MR-based attenuation correction became commercially available (Biograph mMR, Siemens Healthcare, Erlangen, Germany) (9). As of December 2013 more than 50 of these systems have been sold (>40 installed, 10 ordered) in Europe, North America, Asia, and Australia (10).

Clinical applications

Due to its limited availability, technical issues (especially regarding attenuation correction), and the lack of clinical studies, as of today PET/MRI cannot be regarded as an established modality for clinical practice, but rather a promising technology, with clinical and scientific value yet to be defined. Therefore it is essential to identify those applications where PET/MRI provides a clear benefit in comparison to the established reference standards.

Many authors regard PET/CT as the reference standard that sets the benchmark for PET/MRI and thus investigation is to some extent focused on applications where MRI has significant advantages over CT. In this context, promising applications include liver, prostate, or head-and-neck imaging, which take advantage of the excellent soft tissue contrast provided by MRI. In addition to anatomical images, MRI provides functional and quantitative data like diffusion-weighted imaging (DWI), spectroscopy, blood oxygenation level-dependent imaging in functional MRI, T1/T2 mapping and dynamic contrast-enhanced imaging. Consequently, valuable applications of PET/MRI might emerge in the field of multiparametric and quantitative imaging (Fig. 2). For example tumor characterization and response evaluation could benefit from multiparametric imaging as tumors are spatially heterogeneous and dynamically evolving entities that are often not sufficiently characterized by size-based assessment only. In future, multiparametric and quantitative imaging using PET/MRI might play an important role in the management of targeted tumor therapies. On the other hand, in cardiac imaging the benchmark is set by MRI (with the exception of coronary imaging) and thus investigation here is not focused on the question of where PET/

MRI is superior to PET/CT, but rather on where PET/MRI provides added value over stand-alone cardiac MRI.

In addition, PET/MRI offers some unique features like real parallel PET and MRI acquisition that enable certain imaging protocols like integrated functional MRI and dynamic PET after presentation of a stimulus or cardiac stress PET/MRI. In combination with the ionizing radiation-free nature of MRI, parallel acquisition also allows for the continuous acquisition of anatomical images that can be used for motion correction of PET data. Thus, the quality of PET images in applications like cardiac, lung, or bowel imaging can be increased while respiratory and/or electrocardiography-gating can be potentially omitted.

Without the CT component, PET/MRI in comparison to PET/CT eliminates the exposure to X-rays, while higher sensitivity of the PET detection system will potentially allow for a reduction of injected tracer activity in many protocols. In combination, this will lead to a reduced exposure to ionizing radiation (11, 12), which is of particular interest in the imaging of younger patients, in nonfatal disease, and in periodic follow-up examinations.

Oncology

Since the current main application of PET/CT is oncologic imaging, the majority of initial studies on PET/MRI focused on possible advantages in this field. The first reports on PET/MRI in oncologic imaging focused on the feasibility of whole-body PET/MRI for staging purposes in comparison to the clinical standard of PET/CT and found promising results (13–16).

An initial study by Drzezga et al. (13) employing an ^{18}F-fluorodeoxyglucose (FDG) single-injection, dual-imaging protocol consisting of PET/CT and subsequent PET/MRI in 32 patients with different oncologic diseases demonstrated the feasibility of simultaneous PET/MRI in a clinical setting with high image quality and short examination time. Their findings were later confirmed by Quick et al. (14) who found simultaneous PET/MRI to be feasible in a clinical setting in 80 patients with various cancers and inflammatory conditions. While these first studies confirmed the mere feasibility, recently in a retrospective study on 134 patients with non-central nervous system primary malignancies, Catalano et al. (17) showed that PET/MRI provided additional information that was unavailable from PET/CT. In 24 of 134 patients (17.9%) the additional findings even lead to a change in clinical management.

While these first studies concentrated on the new technique in a whole-body approach, further research focused on the applicability in certain tumors and body regions. Given the high soft tissue contrast of MRI as an advantage over CT, PET/MRI is expected to provide more useful information than PET/CT in cancer staging. PET/MRI is expected to provide added value especially in the evaluation of the head and neck, liver, urogenital organs, and the skeleton, regions in which MRI plays a crucial role in the diagnostic process.

Because of its high diagnostic accuracy in the detection and staging of the primary lung tumor and distant metastases, FDG-PET/CT is currently accepted as the modality of choice for staging of non-small cell lung cancer (NSCLC) patients. When compared to FDG-PET/CT, MRI has been proven to provide some advantages in T-staging as well as N-staging performance (18, 19). Hence, it can be expected that MRI in combination with PET may provide a new quality in functional cancer staging in NSCLC patients. Schwenzer et al. (20) recently demonstrated the feasibility of simultaneous PET/MRI for the assessment of pulmonary lesions showing a similar lesion characterization and tumor stage compared to that of FDG-PET/CT. Furthermore, Kohan et al. (21) recently showed that FDG-PET/MRI is comparable to FDG-PET/CT for staging and quantitative assessment of mediastinal NSCLC lymph node metastases.

When proposing PET/MRI as an alternative to PET/CT for whole-body staging the question of its performance in the detection of lung metastases is mandatory, since MRI is known to be associated with low sensitivity for lung lesion detection. Accordingly, in a recent study from Chandarana et al. (22) on 32 patients undergoing PET/CT and PET/MRI, a high sensitivity of PET/MRI for FDG-avid lung lesions (95.6%), yet poor results for FDG-negative lesions was reported. However, for the evaluation of primary lung cancer, PET/MRI offers advantages over PET/CT due to its multiparametric nature allowing for the additional integration of DWI (23, 24). In this setting, PET/MRI in oncologic imaging might not only serve as alternative to PET/CT, it can be used to cross-validate the existing modalities of PET and functional MRI (i.e., DWI).

Imaging of the head and neck region requires a high soft tissue contrast, making MRI the method of choice in this field. However, there is evidence that the additional metabolic information of FDG-PET improves the accuracy of MR examinations in tumors of the head and neck region (25). Hence, PET/MRI appears to be notably valuable for imaging of tumors of the head and neck region (Fig. 3). Since the introduction of PET/MRI scanners, only a limited number of studies dealing with PET/MRI in tumors of the head and neck region have been published. Boss et al. (26) demonstrated feasibility of PET/MRI in eight patients suffering from head and neck cancer with a PET/MRI scanner capable of simultaneous acquisition of PET and MRI data (BrainPET and Magnetom Tim Trio, Siemens Healthcare). They reported an excellent MR image quality, which was not inferior to that of conventional MR scanners. The PET images revealed some streak artifacts, which did not compromise tumor visualization. The SUVs of PET/MRI and PET/CT showed an excellent correlation. Platzek et al. (27) examined 20 patients with histologically proven squamous cell carcinoma of the head and neck region with a sequential PET/MRI system (Ingenuity time-of-flight PET/MRI scanner; Philips Medical Systems, Cleveland, Ohio, USA). They reported superiority of PET/MRI over MRI alone and stand-alone PET in detection of primary tumors and lymph node metastases. No obvious artifacts were found on either PET images or MR images derived from the sequential PET/MRI scanner. In a study on 32 patients with head and neck tumors Varoquaux et al. (28) evaluated image and fusion quality, lesion conspicuity, lesion number and size and found an

equivalent performance for PET/MRI in comparison to PET/CT. Recently, Kubiessa et al. (29) published a comparison of simultaneous PET/MRI with PET/CT on 23 malignant tumors of the head and neck region. They found no statistically significant differences in the diagnostic performance between PET/CT and PET/MRI and recommended further investigations with a larger patient group.

To summarize, PET/MRI of the head and neck region has been shown to be feasible for clinical applications. However, the number of publications regarding this issue is small, warranting further research especially with larger patient groups to identify possible indications for PET/MRI in this field.

For the evaluation of liver metastases, studies on retrospective PET/MRI fusion have already shown promising results (30). The high soft tissue contrast of MRI, as well as the information provided by DWI, enabled a higher detection rate and diagnostic confidence, when compared to PET/CT especially for metastases <1 cm in size. In accordance with these results, a study by Beiderwellen et al. (31) on 70 patients undergoing PET/CT and simultaneously acquired PET/MRI, showed higher lesion conspicuity, as well as diagnostic confidence, using PET/MRI. These results were confirmed by Reiner et al. (32) who reported on 55 patients with suspected liver metastases undergoing PET/CT and PET/MRI using a trimodality system. The authors found that PET/MRI had significantly higher diagnostic confidence in comparison to contrast-enhanced PET/CT. However, higher accuracy of PET/MRI could only be observed in lesions without elevated FDG uptake.

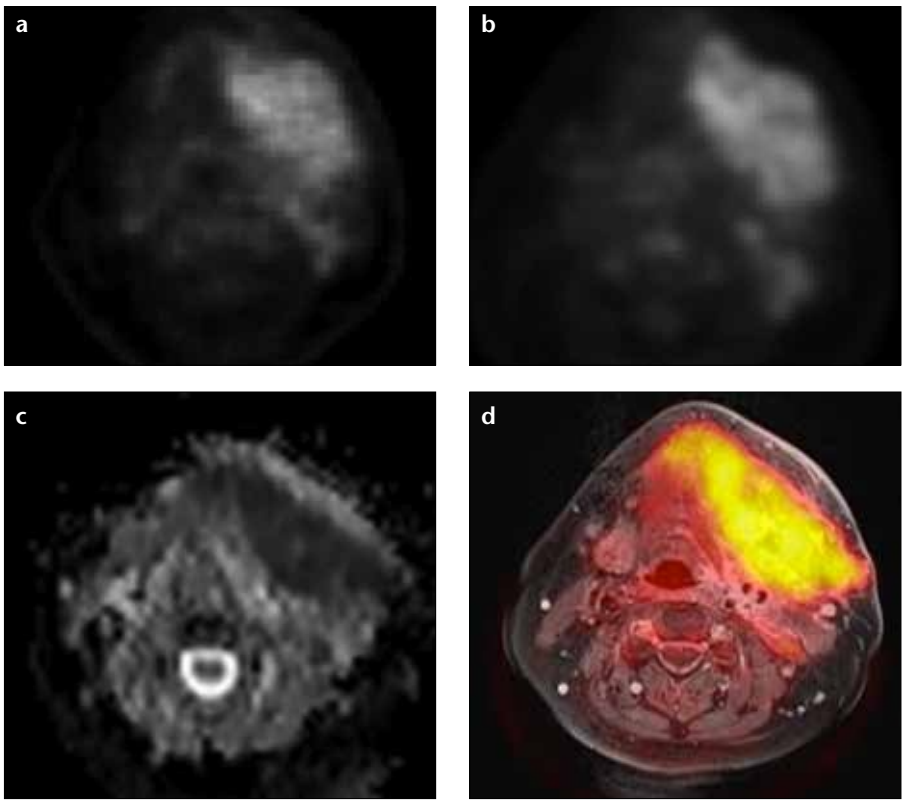

Figure 3. a–d. Images of a large cancer of unknown primary of the head and neck region derived from PET/MRI. This example demonstrates visually comparable quality of PET/CT **(a)** and PET/MRI **(b)** derived PET images. Simultaneous PET/MRI offers the possibility of morphological, functional and metabolic imaging studies in a single examination **(c, d)**. Diffusion-weighted imaging (ADC map; b=[0, 500, 1000]) of the lesion is shown in **(c)**. Fusion of T1-weighted contrast-enhanced image with fat saturation and attenuation-corrected FDG-PET is shown in **(d)**.

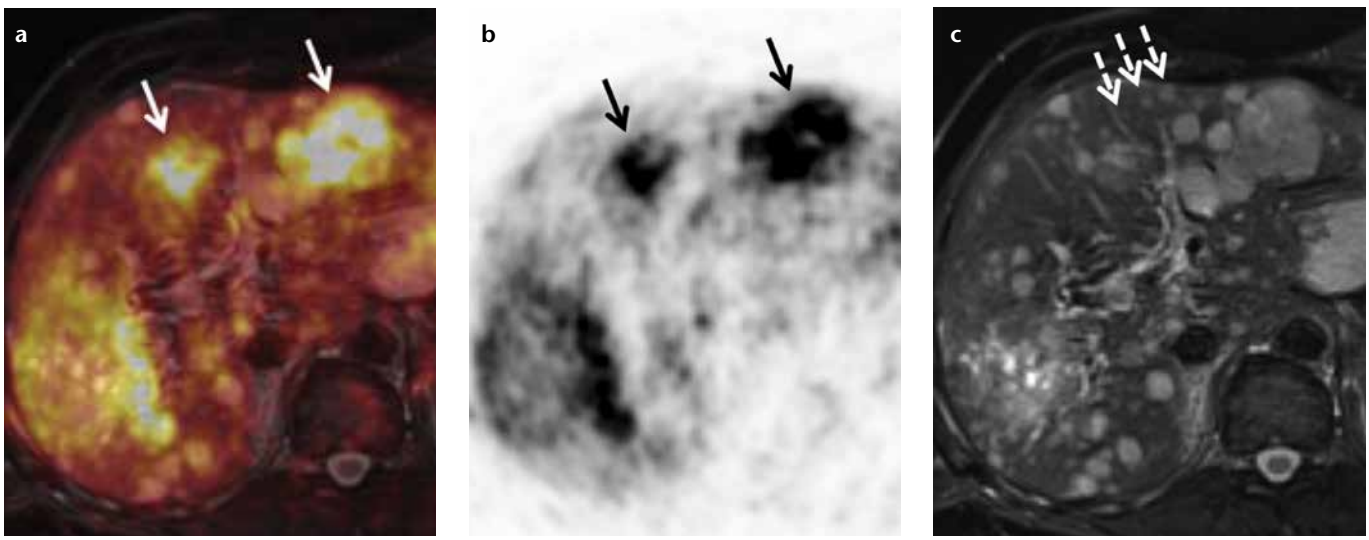

Figure 4. a–c. Simultaneous PET/MRI with ^{68}Ga-DOTATOC in a patient with liver metastases originating from a neuroendocrine tumor (NET) of the pancreas. While PET is very specific and identifies liver metastases due to a NET-specific somatostatin-receptor overexpression (**a**, fusion; **b**, PET; *arrows*), its spatial resolution especially in an organ prone to respiratory motion is limited. T2-weighted MRI allows for correct identification of liver metastases <1 cm in size (**c**, *dashed arrows*). Since CT is less sensitive and less specific than MRI in liver metastases <1 cm in size, the combination of PET and MRI for the assessment of liver metastases appears to be a very powerful combination.

In abdominal applications for special tumor entities the use of more specific non-FDG tracers (^{68}Ga-DOTATOC, ^{18}F-Choline, ^{124}I[MIBG]) is requested by many specialists. For neuroendocrine tumors, a tumor entity associated with early liver metastases, ^{68}Ga-DOTATOC PET/MRI bears an equally high diagnostic potential (Fig. 4). For detection of liver metastases, a study by Schreiter et al. (30) on retrospective fusion PET/MRI in patients with neuroendocrine tumors found that PET/MRI had higher sensitivity (91.2%) in comparison to PET/CT (73.5%). First results by Beiderwellen et al. (16) for simultaneous ^{68}Ga-DOTATOC PET/MRI in eight patients with neuroendocrine tumors are encouraging in demonstrating higher lesion conspicuity as well as diagnostic confidence for PET/MRI.

Due to its high soft tissue contrast, MRI is the method of choice for the evaluation of pelvic malignancies and especially for the diagnosis and staging of prostate cancer (Fig. 5). For the latter, multiparametric PET/MRI has been examined to a large extent with promising results (33). PET imaging of primary and metastatic prostate cancer is usually performed with choline tracers like ^{11}C-choline or ^{18}F-choline and is controversially discussed in the literature, as it shows some limitations in diagnostic accuracy (34). The feasibility of simultaneous PET/MRI in prostate cancer was recently demonstrated for both ^{11}C-choline and ^{18}F-choline. Souvatzoglou et al. (35) compared ^{11}C-choline PET/MRI with ^{11}C-choline PET/CT and described a similar performance of both methods with a better anatomical allocation of bone and pelvic lesions with PET/MRI. Wetter et al. (36) compared ^{18}F-choline PET/MRI with ^{18}F-choline PET/CT with respect to the PET component and reported a comparable image quality of the PET images derived from PET/CT and PET/MRI with identical numbers of PET positive lesions detected in PET/CT and PET/MRI. Regarding primary prostate cancer, PET/MRI allows for precise mapping of PET positive lesions and is therefore clearly advantageous over PET/CT, where an anatomical allocation is difficult due to the reduced tissue contrast of the prostate in CT. In particular, regions of benign prostatic hyperplasia, which can show a pronounced choline uptake, can be accurately identified with PET/MRI and distinguished from tumor-suspicious lesions (15). Including the PET component in multiparametric MRI of the prostate by means of integrated PET/MRI might therefore be a future option regarding primary prostate cancer detection and tumor staging. Therefore, development of new tracers for prostate cancer imaging is necessary and initial results are promising (37).

In the assessment of bone metastases, PET/MRI might equally be a valuable alternative to PET/CT (Fig. 6). Eiber et al. (38) reported on a comparative study on 119 patients undergoing PET/CT and subsequent PET/MRI and found superior results for PET/MRI in the anatomic delineation and allocation using a T1-weighted turbo spin-echo sequence.

Literature regarding applications of PET/MRI in lymphoma and lymph node imaging is scarce to date (Fig. 7). A pilot study conducted by Platzek et al. (39) dealing with response evaluation in malignant lymphoma demonstrated the feasibility of PET/MRI and found a good to excellent PET image quality derived from the PET/MR scanner with sequential acquisition of PET data and MR data. As a perspective, they stated a possibly significant re-

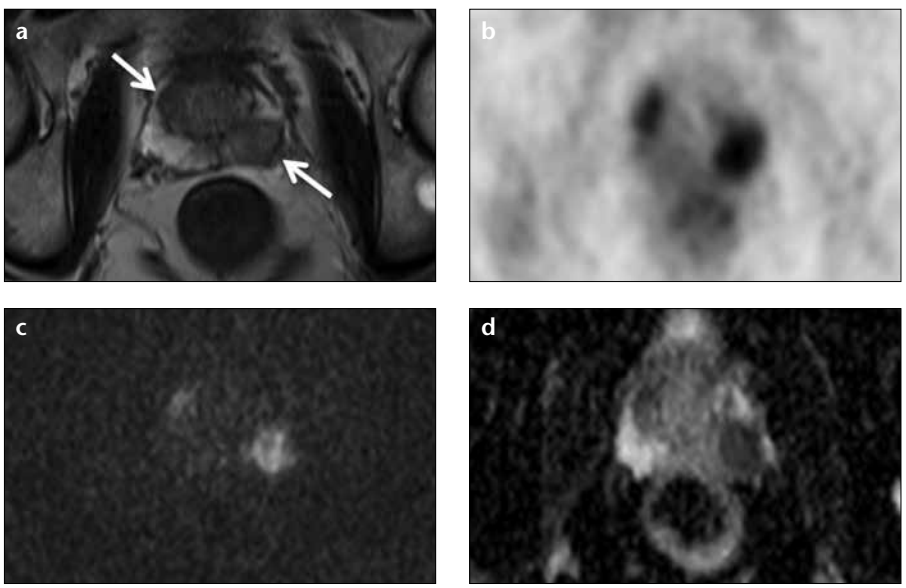

Figure 5. a–d. Combined morphological, functional, and metabolic imaging with simultaneous ^{18}F-choline PET/MRI of a biopsy-proven prostate cancer. T2-weighted image **(a)** showing a hypointense lesion in the left peripheral zone and right transitional zone *(arrows)*. ^{18}F-choline PET image **(b)** derived from PET/MRI. Diffusion-weighted image **(c)** (b=1500) with high signal in the tumor lesions. ADC map **(d)** with corresponding low signal.

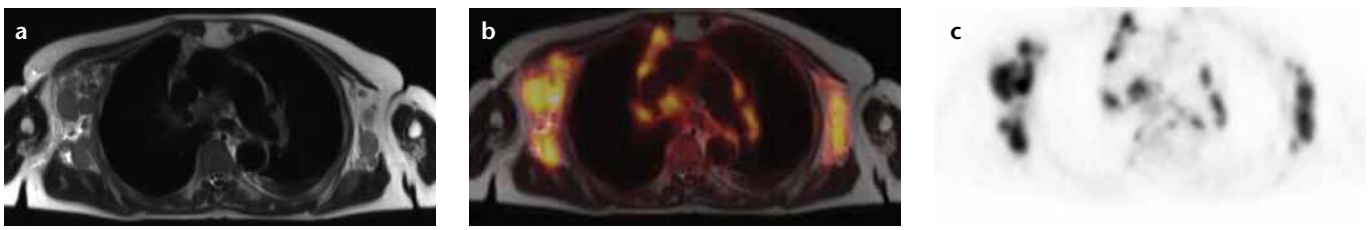

Figure 6. a–c. Simultaneous FDG-PET/MRI in a 72-year-old patient with an initial diagnosis of highly malignant B-cell type non-Hodgkin lymphoma. The anatomical dataset shows multiple enlarged axillary, mediastinal, as well as hilar lymph nodes (**a,** T2-weighted HASTE) with elevated FDG-uptake in PET (**b,** fusion; **c,** FDG-PET).

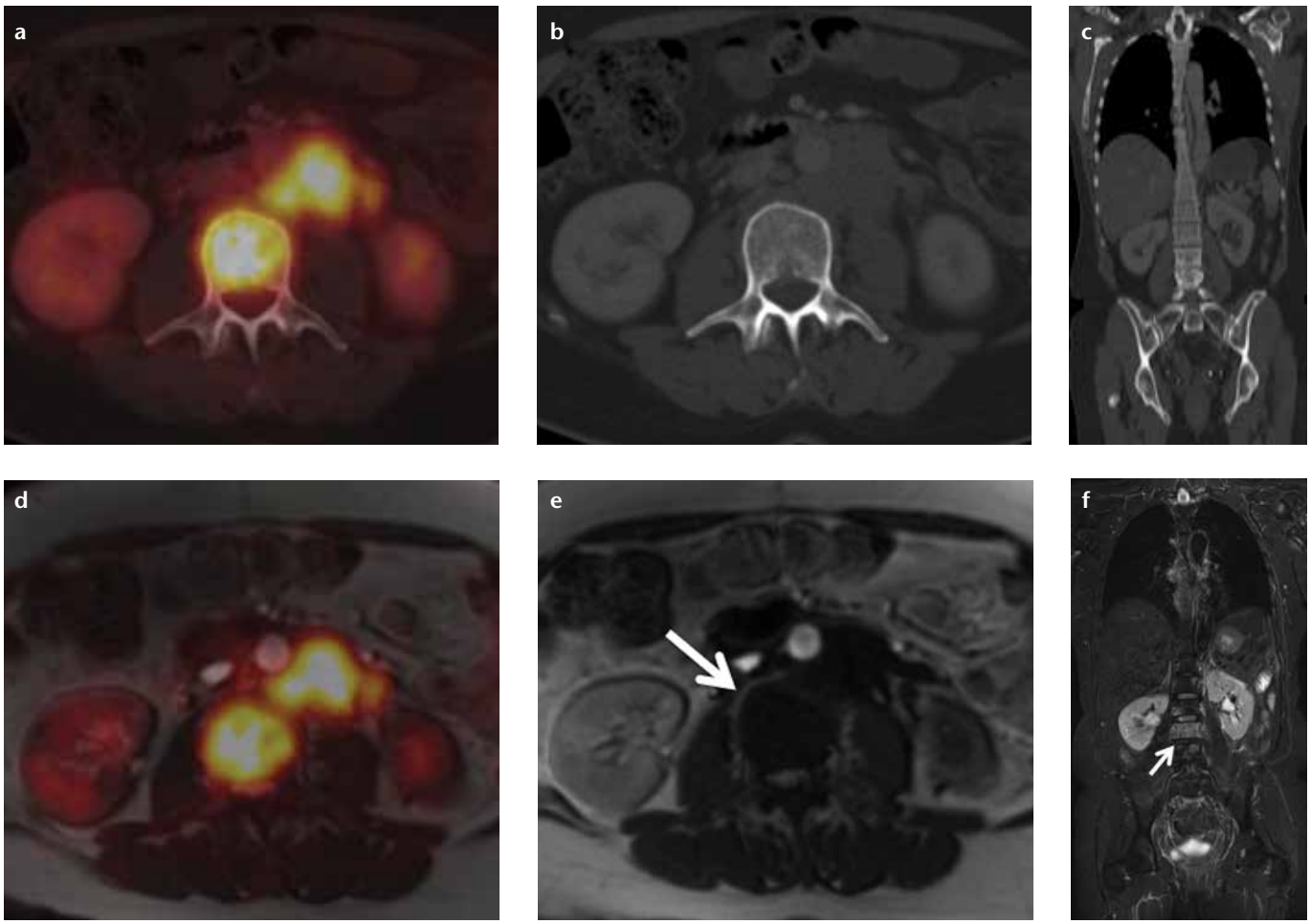

Figure 7. a–f. A patient with bone metastases originating from ovarian cancer and local bone marrow infiltration in the lumbar spine. While in FDG-PET/CT **(a–c)** the bone marrow infiltration is only detectable in PET **(a)** and shows no osseous destruction in CT **(b, c)**, in FDG-PET/MRI **(d–f)** the infiltration is detectable both in PET **(d)** and in MRI due to a low signal in T1-weighted sequences (**e,** *arrow*) and high signal in T2-weighted sequences (**f,** *arrow*). Especially in patients undergoing chemotherapy bone metastases/bone marrow infiltrates might not be FDG-avid and therefore not detectable in PET/CT. In this case PET/MRI might represent an advantage in whole-body imaging.

duction of the cumulative radiation dose with replacement of CT by MRI. Regarding lymph node imaging, Appenzeller et al. (40) reported superiority of low-dose PET/CT over PET/MRI regarding lesion conspicuity of lymph nodes and found that PET/MRI did not match diagnostic accuracy of low dose PET/CT.

Cardiovascular

Noninvasive cardiac MRI has evolved into the standard of reference in many aspects. Due to excellent soft tissue contrast, good spatial resolution, and contrast-enhanced imaging techniques, MRI is a clinically well-established tool for myocardial tissue classification. Cine-imaging techniques allow for the assessment of myocardial wall-motion at rest and under stress as well as the assessment of ventricular and valvular function. Myocardial rest and stress perfusion can be estimated with intravenous contrast-agents, and hemodynamics can be measured and visualized with two- and three-dimensional flow imaging.

Cardiac and respiratory motion, multidirectional blood flow, and involvement of small anatomical structures like heart valves make cardiac MRI a complex task requiring advanced image acquisition techniques, being potentially more sensitive to inhomogeneity of the magnetic field. However, a recent study and several case reports have proved the technical feasibility and good image quality of cardiac PET/MRI with FDG on an integrated scanner (41–44).

Cardiac PET imaging with FDG is complicated by strong glucose uptake in normal myocardium that varies with the availability of blood glucose and free fatty acids. This requires special patient preparation techniques such as increasing the availability of blood glucose and shifting myocardial metabolism to glucose consumption, which results in a homogeneous FDG uptake in the normal myocardium as required in viability imaging. Other techniques increase the availability of free fatty acids and suppress FDG uptake in the normal myocardium as required in the imaging of cardiac inflammation or tumors.

While cardiac MRI utilizing late gadolinium-enhancement has been shown to accurately demonstrate myocardial necrosis and scarring, some authors regard PET match/mismatch imaging with FDG and a perfusion tracer like ^{13}N-Ammonia as the reference standard for myocardial viability (45).

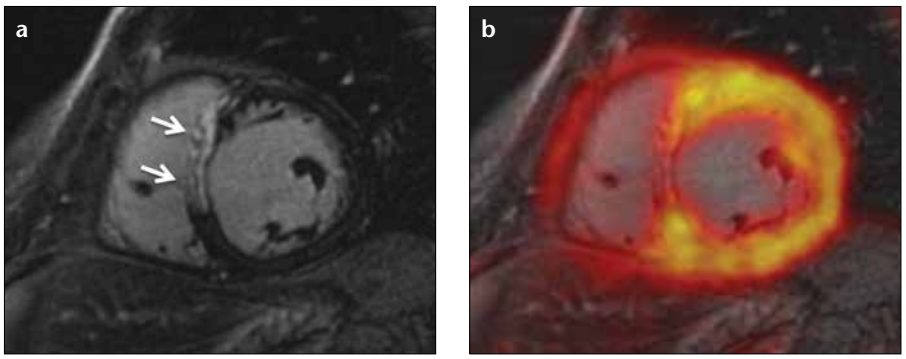

Figure 8. a, b. A patient with acute myocardial infarction due to occlusion of the left anterior descending (LAD) coronary artery. Late gadolinium-enhancement reveals transmural septal infarction (**a,** *arrows*) that corresponds to a clearly reduced FDG uptake **(b)**.

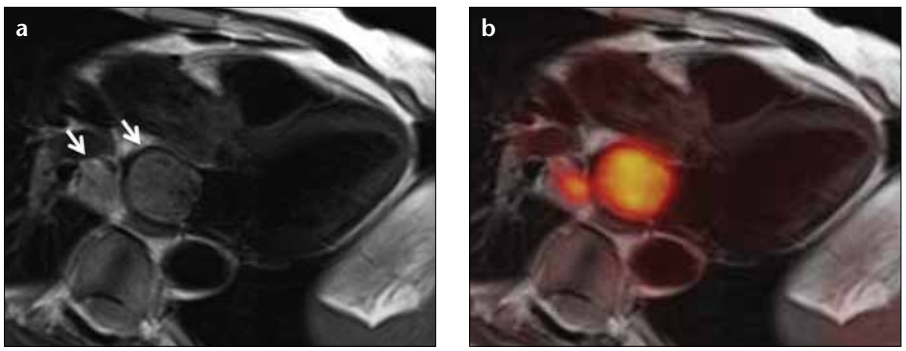

Figure 9. a, b. A patient with central non-small cell lung cancer infiltrating the left atrium via the lower right pulmonary vein (**a,** *arrows*). MR images provide excellent anatomical soft tissue contrast and allow for the detection and quantification of potential impairment of functional parameters like ventricular or valvular function or blood flow. Simultaneous FDG-PET can help in determination of malignancy or differentiation of vital tumor from necrotic tissue or thrombus **(b)**.

Several studies, including one PET/MRI study, have shown close agreement between FDG-PET and late gadolinium-enhancement (43, 46, 47) (Fig. 8). However, there is some evidence that reduced FDG uptake might not only be present in myocardial necrosis or scarring, but also in jeopardized but viable myocardium after acute ischemia, and thus could correspond to the area-at-risk (43, 48). If this can be confirmed by further studies, integrated FDG-PET and late gadolinium-enhancement would retrospectively allow for the assessment of the salvage-area after recanalization of acute myocardial infarction.

PET imaging with FDG is being increasingly recognized as a valuable tool in the assessment of various inflammatory diseases (49), and a case report by White et al. (44) has already demonstrated the feasibility of PET/MRI in cardiac sarcoidosis. Cardiac MRI has shown to provide good diagnostic performance in acute myocarditis but is still unsatisfactory in the detection of chronic myocarditis (50). Furthermore, T2-weighted images, which are particularly important for the differentiation between acute and chronic myocardial inflammation, are prone to artifacts and often do not yield a consistent image quality, especially in patients with arrhythmia and other motion artifacts (51, 52). In contrast, with FDG-PET one can directly visualize the metabolic activity of inflammatory infiltrates and thus detect myocarditis in the acute and chronic state. Due to the quantitative nature of PET imaging, FDG-PET might also be useful to assess inflammatory myocardial disease activity for therapy response evaluation (53). Besides myocarditis, detection and monitoring of cardiac sarcoidosis might emerge as an important application of PET/MRI. Cardiac involvement is a strong predictor of worse outcome in sarcoidosis, and early detection as well as close monitoring, including the differentiation between active and chronic cardiac sarcoidosis, might help in the management of this potentially fatal complication. Several case reports have demonstrated the potential of integrated FDG-PET/MRI in the imaging of cardiac sarcoidosis (44, 54, 55).

Considering the impact of PET/CT in oncology, imaging of cardiac tumors is an obvious application of PET/MRI (Fig. 9). As of today, no corresponding reports or studies have been published. However, a PET/CT study from Rahbar et al. (56) showed that FDG-PET/CT can help in determination of cardiac malignancy and metastases of malignant cardiac tumors. While cardiac MRI is already the noninvasive reference standard for differential diagnosis and local staging of cardiac tumors, an additional perspective on tumor metabolism could probably help in evaluation of tumor dignity and detection of occult tumor sites.

The imaging of vulnerable atherosclerotic plaques seems to be another promising application of PET/MRI. While Joshi et al. (57) have recently demonstrated the identification of ruptured and high-risk coronary atherosclerotic plaques using ^{18}F-fluoride PET/CT in a remarkable prospective trial, the feasibility of plaque imaging with integrated PET/MRI has already been shown by Ripa et al. (58).

Central nervous system

For several reasons PET/MRI of the brain is unique: First, there are comparatively few sources of involuntary cranial motion (e.g., pulsation, tremor). Therefore, sequential scanning and fusion is feasible in many cases if patients cooperate, and fully integrated PET/MRI is only needed in the simultaneous imaging of temporally coupled processes, like the regional consumption of oxygen and glucose in functional PET/MRI studies. Furthermore, the high symmetry and extremely low deformability of the head facilitate post-hoc rigid motion correction and co-registration with software-based methods. The comparably small dimension of the head already allowed for integrated PET/MRI with PET inserts in standard MR scanners, when integrated whole-body devices were not yet available. The geometry of the head also enables homogenous magnetic fields in ultra-high field MRI, which can provide high quality MR data for fusion with

PET. Finally, for well-known reasons MRI is superior to CT in many applications of central nervous system imaging, which makes PET/MRI a desirable alternative to PET/CT in the imaging of neurologic diseases.

The parallel image acquisition in integrated PET/MRI can be exploited to track patient motion (e.g., in uncooperative patients or patients with tremor) with fast MRI sequences and use this information to remove motion from the simultaneously acquired PET images. The feasibility of this so-called MRI-assisted PET motion correction technique has been demonstrated by Catana et al. (59), and meanwhile, it has become commercially available (Brain COMPASS, Siemens Healthcare).

MRI is the first-line method of choice in many applications of neuro-oncologic imaging. It allows for superb visualization of tumors and provides advanced techniques like DWI, dynamic contrast-enhanced imaging, functional MRI and MR spectroscopy. However, there are still limitations such as the correct classification of gliomas, the spread of glioma cells along white matter tracts and tumor response evaluation to therapy. PET could add a molecular perspective to visualize specific processes like the secretion of matrix-metalloproteinases by infiltrating glioma cells (60) or the turnover of radiolabeled aminoacids in vital tumor cells (61). A study by Boss et al. (62) in ten patients with intracranial masses demonstrated that tumor assessment with ^{11}C-methionine and ^{68}Ga-DOTATOC using PET/MRI was feasible with diagnostic image quality compared to PET/CT. The feasibility of integrated PET/MRI, including advanced techniques such as arterial spin labeling and MR spectroscopy, was demonstrated in another study in 50 patients with intracranial masses, head and upper neck tumors, or neurodegenerative diseases (63). These results encourage the translation of existing preclinical findings into the clinical routine, such as the forecast of glioblastoma therapy response in rats using PET and MRI (64). A study by Bisdas et al. (65) demonstrated the feasibility of simultaneous ^{11}C-methionine PET and MR spectroscopy for purposes of tumor grading in 28 consecutive patients with gliomas. This study found that, although partially correlated, ^{11}C-methionine PET and MR spectroscopy show spatial distribution differences that should be taken into account when planning surgical sampling.

In a study applying different imaging modalities in patients with dementia, the combination of FDG-PET and MRI was superior to the unimodal approach with an accuracy rate of 94% for the differentiation of Alzheimer's disease and frontotemporal lobar degeneration (66). Also, a case report showing colocalized atrophy and hypometabolism in the frontal lobe demonstrated the feasibility of integrated PET/MRI in a patient with frontotemporal dementia (67). In near future, amyloid and tau tangle specific tracers are expected to further improve the diagnosis of Alzheimer's disease using integrated PET/MRI (68).

Salamon et al. (69) recently demonstrated that the incorporation of coregistered FDG-PET and MRI images into presurgical evaluation improved the noninvasive identification and successful surgical treatment of patients with cortical dysplasia.

Pediatric

As already mentioned, integrated PET/MRI holds great potential in the imaging of pediatric patients and young adults with potentially curable disease. Jones and Budinger (12) even proposed that the combination of ionizing radiation-free MRI with short-lived PET nuclides such as ^{15}O or ^{11}C could allow for integrated PET/MRI at acceptable absorbed doses of radiation, creating a potential for the imaging of the human fetus *in vivo*. Hirsch et al. (11) reported their initial experience after 21 PET/MRI studies in 15 children with multifocal malignant diseases. They found the effective dose of a PET/MRI scan to be only about 20% of the equivalent PET/CT scan. Although they reported a significantly longer examination time compared to PET/CT, they concluded that PET/MRI was stable, reliable, and generated great additional value. A retrospective study by Mueller et al. (70) compared 21 separately acquired FDG-PET and MRI scans in 15 pediatric patients with histiocytosis. They found combined PET and MRI to be pivotal due to a decreased false-negative rate during primary staging and a lower number of false-positive findings in lesion follow-up after chemotherapy.

Conclusion

With the commercial availability of integrated whole-body PET/MRI scanners, true simultaneous PET and MRI has become the objective of worldwide scientific research. Various studies have demonstrated the feasibility of simultaneous PET/MRI in many applications, from examinations of the brain to hybrid cardiac imaging. Other studies have found added value of integrated PET/MRI compared to PET/CT or stand-alone MRI, such as MR-based motion correction of PET data, lower radiation exposure, and multiparametric assessment of pathologies. However, there are problems like inaccurate attenuation correction due to missing bone segmentation and longer examination times that require further technical improvements. Although research on integrated PET/MRI is still in its infancy, especially those applications that demand either multiparametric imaging capabilities, high soft tissue contrast, and/or lower radiation dose already seem to benefit from this novel hybrid modality.

From the present point of view, future development of PET/MRI will be driven by multiple important factors: Further clinical studies will have to prove an added value of PET/MRI over the current standards of care to justify the investments in this expensive technology. Concise PET/MR imaging protocols and workflows need to be developed, that preserve the added value of PET/MRI on the evidence of reasonable cost-benefit ratios. Ongoing technical innovation on scanner hard- and software is needed to eliminate current issues like attenuation correction, and fully exploit new opportunities like MR-based motion correction. Also, the worldwide availability of PET/MRI scanners needs to grow significantly to become a common standard of care outside the highly specialized centers, and agreements on adequate refunding of PET/MRI examinations need to be reached. Finally, the translation of new PET tracers from preclinical evaluation into clinical applications will

notably foster the entire field of hybrid PET imaging, including PET/MRI.

Conflict of interest disclosure

The authors declared no conflicts of interest.

References

1. Slomka PJ, Baum RP. Multimodality image registration with software: state-of-the-art. Eur J Nucl Med Mol Imaging 2009; 36 (Suppl 1):S44–S55. [CrossRef]
2. Zaidi H, Ojha N, Morich M, et al. Design and performance evaluation of a whole-body Ingenuity TF PET-MRI system. Phys Med Biol 2011; 56:3091–3106. [CrossRef]
3. Veit-Haibach P, Kuhn FP, Wiesinger F, Delso G, von Schulthess G. PET-MR imaging using a tri-modality PET/CT-MR system with a dedicated shuttle in clinical routine. MAGMA 2013; 26:25–35. [CrossRef]
4. Pichler BJ, Swann BK, Rochelle J, Nutt RE, Cherry SR, Siegel SB. Lutetium oxyorthosilicate block detector readout by avalanche photodiode arrays for high resolution animal PET. Phys Med Biol 2004; 49:4305–4319. [CrossRef]
5. Yoon HS, Ko GB, Kwon SI, et al. Initial results of simultaneous PET/MRI experiments with an MRI-compatible silicon photomultiplier PET scanner. J Nucl Med 2012; 53:608–614. [CrossRef]
6. Martinez-Möller A, Souvatzoglou M, Delso G, et al. Tissue classification as a potential approach for attenuation correction in whole-body PET/MRI: evaluation with PET/CT data. J Nucl Med 2009; 50:520–526. [CrossRef]
7. Ma J. Dixon techniques for water and fat imaging. J Magn Reson Imaging 2008; 28:543–558. [CrossRef]
8. Kim JH, Lee JS, Song IC, Lee DS. Comparison of segmentation-based attenuation correction methods for PET/MRI: evaluation of bone and liver standardized uptake value with oncologic PET/CT data. J Nucl Med 2012; 53:1878–1882. [CrossRef]
9. Delso G, Fürst S, Jakoby B, et al. Performance measurements of the Siemens mMR integrated whole-body PET/MR scanner. J Nucl Med 2011; 52:1914–1922. [CrossRef]
10. Quick HH. Integrated PET/MR. J Magn Reson Imaging 2013; 39:243–258. [CrossRef]
11. Hirsch FW, Sattler B, Sorge I, et al. PET/MR in children. Initial clinical experience in paediatric oncology using an integrated PET/MR scanner. Pediatr Radiol 2013; 43:860–875. [CrossRef]
12. Jones T, Budinger TF. The potential for low-dose functional studies in maternal-fetal medicine using PET/MR imaging. J Nucl Med 2013; 54:2016–2017. [CrossRef]
13. Drzezga A, Souvatzoglou M, Eiber M, et al. First clinical experience with integrated whole-body PET/MR: comparison to PET/CT in patients with oncologic diagnoses. J Nucl Med 2012; 53:845–855. [CrossRef]
14. Quick HH, von Gall C, Zeilinger M, et al. Integrated whole-body PET/MR hybrid imaging: clinical experience. Invest Radiol 2013; 48:280–289. [CrossRef]
15. Wetter A, Lipponer C, Nensa F, et al. Simultaneous 18F choline positron emission tomography/magnetic resonance imaging of the prostate: initial results. Invest Radiol 2013; 48:256–262. [CrossRef]
16. Beiderwellen KJ, Poeppel TD, Hartung-Knemeyer V, et al. Simultaneous 68Ga-DOTATOC PET/MRI in patients with gastroenteropancreatic neuroendocrine tumors: initial results. Invest Radiol 2013; 48:273–279. [CrossRef]
17. Catalano OA, Rosen BR, Sahani DV, et al. Clinical impact of PET/MR imaging in patients with cancer undergoing same-day PET/CT: initial experience in 134 patients-a hypothesis-generating exploratory study. Radiology 2013; 269:857–869. [CrossRef]
18. Plathow C, Aschoff P, Lichy MP, et al. Positron emission tomography/computed tomography and whole-body magnetic resonance imaging in staging of advanced nonsmall cell lung cancer--initial results. Invest Radiol 2008; 43:290–297. [CrossRef]
19. Ohno Y, Koyama H, Yoshikawa T, et al. N stage disease in patients with non-small cell lung cancer: efficacy of quantitative and qualitative assessment with STIR turbo spin-echo imaging, diffusion-weighted MR imaging, and fluorodeoxyglucose PET/CT. Radiology 2011; 261:605–615. [CrossRef]
20. Schwenzer NF, Schraml C, Müller M, et al. Pulmonary lesion assessment: comparison of whole-body hybrid MR/PET and PET/CT imaging--pilot study. Radiology 2012; 264:551–558. [CrossRef]
21. Kohan AA, Kolthammer JA, Vercher-Conejero JL, et al. N staging of lung cancer patients with PET/MRI using a three-segment model attenuation correction algorithm: initial experience. Eur Radiol 2013; 23:3161–3169. [CrossRef]
22. Chandarana H, Heacock L, Rakheja R, et al. Pulmonary nodules in patients with primary malignancy: comparison of hybrid PET/MR and PET/CT imaging. Radiology 2013; 268:874–881. [CrossRef]
23. Heusch P, Köhler J, Wittsack HJ, et al. Hybrid [(18)F]-FDG PET/MRI including non-Gaussian diffusion-weighted imaging (DWI): preliminary results in non-small cell lung cancer (NSCLC). Eur J Radiol 2013; 82:2055–2060. [CrossRef]
24. Heusch P, Buchbender C, Köhler J, et al. Correlation of the apparent diffusion coefficient (ADC) with the standardized uptake value (SUV) in hybrid 18F-FDG PET/MRI in non-small cell lung cancer (NSCLC) lesions: initial results. Rofo 2013; 185:1056–1062. [CrossRef]
25. Mak D, Corry J, Lau E, Rischin D, Hicks RJ. Role of FDG-PET/CT in staging and follow-up of head and neck squamous cell carcinoma. Q J Nucl Med Mol Imaging 2011; 55:487–499.
26. Boss A, Stegger L, Bisdas S, et al. Feasibility of simultaneous PET/MR imaging in the head and upper neck area. Eur Radiol 2011; 21:1439–1446. [CrossRef]
27. Platzek I, Beuthien-Baumann B, Schneider M, et al. PET/MRI in head and neck cancer: initial experience. Eur J Nucl Med Mol Imaging 2013; 40:6-11. [CrossRef]
28. Varoquaux A, Rager O, Poncet A, et al. Detection and quantification of focal uptake in head and neck tumours: (18)F-FDG PET/MR versus PET/CT. Eur J Nucl Med Mol Imaging 2013; 41(3):462-475. [CrossRef]
29. Kubiessa K, Purz S, Gawlitza M, et al. Initial clinical results of simultaneous (18) F-FDG PET/MRI in comparison to (18) F-FDG PET/CT in patients with head and neck cancer. Eur J Nucl Med Mol Imaging 2014; 41:639–648. [CrossRef]
30. Schreiter NF, Nogami M, Steffen I, et al. Evaluation of the potential of PET-MRI fusion for detection of liver metastases in patients with neuroendocrine tumours. Eur Radiol 2012; 22:458–467. [CrossRef]
31. Beiderwellen K, Gomez B, Buchbender C, et al. Depiction and characterization of liver lesions in whole body [18F]-FDG PET/MRI. Eur J Radiol 2013; 82:e669–e675. [CrossRef]
32. Reiner CS, Stolzmann P, Husmann L, et al. Protocol requirements and diagnostic value of PET/MR imaging for liver metastasis detection. Eur J Nucl Med Mol Imaging 2014; 41:649–658. [CrossRef]
33. Murphy G, Haider M, Ghai S, Sreeharsha B. The expanding role of MRI in prostate cancer. AJR Am J Roentgenol 2013; 201:1229–1238. [CrossRef]
34. Bauman G, Belhocine T, Kovacs M, Ward A, Beheshti M, Rachinsky I. 18F-fluorocholine for prostate cancer imaging: a systematic review of the literature. Prostate Cancer Prostatic Dis 2012; 15:45–55. [CrossRef]
35. Souvatzoglou M, Eiber M, Takei T, et al. Comparison of integrated whole-body [11C]choline PET/MR with PET/CT in patients with prostate cancer. Eur J Nucl Med Mol Imaging 2013; 40:1486–1499. [CrossRef]
36. Wetter A, Lipponer C, Nensa F, et al. Evaluation of the PET component of simultaneous [(18)F]choline PET/MRI in prostate cancer: comparison with [(18)F]choline PET/CT. Eur J Nucl Med Mol Imaging 2014; 41:79–88. [CrossRef]
37. Afshar-Oromieh A, Malcher A, Eder M, et al. PET imaging with a [68Ga]gallium-labelled PSMA ligand for the diagnosis of prostate cancer: biodistribution in humans and first evaluation of tumour lesions. Eur J Nucl Med Mol Imaging 2013; 40:486–495. [CrossRef]
38. Eiber M, Takei T, Souvatzoglou M, et al. Performance of whole-body integrated 18F-FDG PET/MR in comparison to PET/CT for evaluation of malignant bone lesions. J Nucl Med 2013; 55:191–197. [CrossRef]

39. Platzek I, Beuthien-Baumann B, Langner J, et al. PET/MR for therapy response evaluation in malignant lymphoma: initial experience. MAGMA 2013; 26:49–55. [CrossRef]
40. Appenzeller P, Mader C, Huellner MW, et al. PET/CT versus body coil PET/MRI: how low can you go? Insights Imaging 2013; 4:481–490. [CrossRef]
41. Schlosser T, Nensa F, Mahabadi AA, Poeppel TD. Hybrid MRI/PET of the heart: a new complementary imaging technique for simultaneous acquisition of MRI and PET data. Heart 2012; 99:351–352. [CrossRef]
42. Ibrahim T, Nekolla SG, Langwieser N, et al. Simultaneous positron emission tomography/magnetic resonance imaging identifies sustained regional abnormalities in cardiac metabolism and function in stress-induced transient midventricular ballooning syndrome. Circulation 2012; 126:e324–e326. [CrossRef]
43. Nensa F, Poeppel TD, Beiderwellen K, et al. Hybrid PET/MR imaging of the heart: feasibility and initial results. Radiology 2013; 268:366–373. [CrossRef]
44. White JA, Rajchl M, Butler J, Thompson RT, Prato FS, Wisenberg G. Active cardiac sarcoidosis: first clinical experience of simultaneous positron emission tomography-magnetic resonance imaging for the diagnosis of cardiac disease. Circulation 2013; 127:e639–e641. [CrossRef]
45. Camici PG, Prasad SK, Rimoldi OE. Stunning, hibernation, and assessment of myocardial viability. Circulation 2008; 117:103–114. [CrossRef]
46. Hunold P, Brandt-Mainz K, Freudenberg L, et al. Evaluation of myocardial viability with contrast-enhanced magnetic resonance imaging--comparison of the late enhancement technique with positronemission tomography. Fortschr Röntgenstr 2002; 174:867–873. [CrossRef]
47. Higuchi T, Nekolla SG, Jankaukas A, et al. Characterization of normal and infarcted rat myocardium using a combination of small-animal PET and clinical MRI. J Nucl Med 2007; 48:288–294.
48. Nensa F, Poeppel TD, Beiderwellen KJ, et al. Cardiac PET/MRI with 18F-FDG: Feasibility and initial results in patients with acute myocardial infarction. Paper presented at: 2013 Annual Meeting of the Radiological Society of North America; December 3, 2013; Chicago, USA.
49. Haroon A, Zumla A, Bomanji J. Role of fluorine 18 fluorodeoxyglucose positron emission tomography-computed tomography in focal and generalized infectious and inflammatory disorders. Clin Infect Dis 2012; 54:1333–1341. [CrossRef]
50. Lurz P, Eitel I, Adam J, et al. Diagnostic performance of CMR imaging compared with EMB in patients with suspected myocarditis. JACC Cardiovasc Imaging 2012; 5:513–524. [CrossRef]
51. Friedrich MG, Sechtem U, Schulz-Menger J, et al. Cardiovascular magnetic resonance in myocarditis: A JACC White Paper. J Am Coll Cardiol 2009; 53:1475–1487. [CrossRef]
52. Carbone I, Friedrich MG. Myocardial edema imaging by cardiovascular magnetic resonance: current status and future potential. Curr Cardiol Rep 2012; 14:1–6. [CrossRef]
53. Sobic-Saranovic DP, Grozdic IT, Videnovic-Ivanov J, et al. Responsiveness of FDG PET/CT to treatment of patients with active chronic sarcoidosis. Clin Nucl Med 2013; 38:516–521. [CrossRef]
54. O'Meara C, Menezes LJ, White SK, Wicks E, Elliott P. Inital experience of imaging cardiac sarcoidosis using hybrid PET-MR - a technologist's case study. J Cardiovasc Magn Reson 2013; 15:T1.
55. Schneider S, Batrice A, Rischpler C, Eiber M, Ibrahim T, Nekolla SG. Utility of multimodal cardiac imaging with PET/MRI in cardiac sarcoidosis: Implications for diagnosis, monitoring and treatment. Eur Heart J 2014; 35:312. [CrossRef]
56. Rahbar K, Seifarth H, Schäfers M, et al. Differentiation of malignant and benign cardiac tumors using 18F-FDG PET/CT. J Nucl Med 2012; 53:856–863. [CrossRef]
57. Joshi NV, Vesey AT, Williams MC, et al. 18F-fluoride positron emission tomography for identification of ruptured and high-risk coronary atherosclerotic plaques: a prospective clinical trial. Lancet 2013; 383:705–713. [CrossRef]
58. Ripa RS, Knudsen A, Hag AM, et al. Feasibility of simultaneous PET/MR of the carotid artery: first clinical experience and comparison to PET/CT. Am J Nucl Med Mol Imaging 2013; 3:361–371.
59. Catana C, Benner T, van der Kouwe A, et al. MRI-assisted PET motion correction for neurologic studies in an integrated MR-PET scanner. J Nucl Med 2011; 52:154–161. [CrossRef]
60. Price SJ, Gillard JH. Imaging biomarkers of brain tumour margin and tumour invasion. Br J Radiol 2011; 84 (Spec No 2):S159–S167. [CrossRef]
61. Jacobs AH, Thomas A, Kracht LW, et al. 18F-fluoro-L-thymidine and 11C-methylmethionine as markers of increased transport and proliferation in brain tumors. J Nucl Med 2005; 46:1948–1958.
62. Boss A, Bisdas S, Kolb A, et al. Hybrid PET/MRI of intracranial masses: initial experiences and comparison to PET/CT. J Nucl Med 2010; 51:1198–1205. [CrossRef]
63. Schwenzer NF, Stegger L, Bisdas S, et al. Simultaneous PET/MR imaging in a human brain PET/MR system in 50 patients--current state of image quality. Eur J Radiol 2012; 81:3472–3478. [CrossRef]
64. Corroyer-Dulmont A, Pérès EA, Petit E, et al. Detection of glioblastoma response to temozolomide combined with bevacizumab based on µMRI and µPET imaging reveals [18F]-fluoro-L-thymidine as an early and robust predictive marker for treatment efficacy. Neuro Oncol 2013; 15:41–56. [CrossRef]
65. Bisdas S, Ritz R, Bender B, et al. Metabolic mapping of gliomas using hybrid MR-PET imaging: feasibility of the method and spatial distribution of metabolic changes. Invest Radiol 2013; 48:295–301. [CrossRef]
66. Dukart J, Mueller K, Horstmann A, et al. Combined evaluation of FDG-PET and MRI improves detection and differentiation of dementia. PLoS One 2011; 6:e18111. [CrossRef]
67. Moodley KK, Minati L, Barnes A, Dickson JC, Ell PJ, Chan D. Simultaneous PET/MRI in frontotemporal dementia. Eur J Nucl Med Mol Imaging 2013; 40:468–469. [CrossRef]
68. Becker GA, Ichise M, Barthel H, et al. PET quantification of 18F-florbetaben binding to β-amyloid deposits in human brains. J Nucl Med 2013; 54:723–731. [CrossRef]
69. Salamon N, Kung J, Shaw SJ, et al. FDG-PET/MRI coregistration improves detection of cortical dysplasia in patients with epilepsy. Neurology 2008; 71:1594–1601. [CrossRef]
70. Mueller WP, Melzer HI, Schmid I, Coppenrath E, Bartenstein P, Pfluger T. The diagnostic value of 18F-FDG PET and MRI in paediatric histiocytosis. Eur J Nucl Med Mol Imaging 2013; 40:356–363. [CrossRef]